UCRL-18480

Cy. 2

RECEIVED
[illegible]
[illegible]
JAN 1, 1969

LIBRARY AND
DOCUMENTS SECTION

A STUDY OF THE OPTICAL PROPERTIES AND OF THE PHYSICAL ADSORPTION OF GASES ON SILVER SINGLE CRYSTAL SURFACES BY LOW ENERGY ELECTRON DIFFRACTION AND ELLIPSOMETRY

R. F. Steiger, J. M. Morabito, Jr., G. A. Somorjai and R. H. Muller

October 1968

TWO-WEEK LOAN COPY

This is a Library Circulating Copy which may be borrowed for two weeks. For a personal retention copy, call Tech. Info. Division, Ext. 5545

UCRL-18480 Cy. 2

LAWRENCE RADIATION LABORATORY
UNIVERSITY of CALIFORNIA BERKELEY

DISCLAIMER

This document was prepared as an account of work sponsored by the United States Government. While this document is believed to contain correct information, neither the United States Government nor any agency thereof, nor the Regents of the University of California, nor any of their employees, makes any warranty, express or implied, or assumes any legal responsibility for the accuracy, completeness, or usefulness of any information, apparatus, product, or process disclosed, or represents that its use would not infringe privately owned rights. Reference herein to any specific commercial product, process, or service by its trade name, trademark, manufacturer, or otherwise, does not necessarily constitute or imply its endorsement, recommendation, or favoring by the United States Government or any agency thereof, or the Regents of the University of California. The views and opinions of authors expressed herein do not necessarily state or reflect those of the United States Government or any agency thereof or the Regents of the University of California.

Submitted to Surface Science

UCRL-18480
Preprint

UNIVERSITY OF CALIFORNIA
Lawrence Radiation Laboratory
Berkeley, California

AEC Contract No. W-7405-eng-48

A STUDY OF THE OPTICAL PROPERTIES AND OF THE PHYSICAL ADSORPTION OF GASES ON SILVER SINGLE CRYSTAL SURFACES BY LOW ENERGY ELECTRON DIFFRACTION AND ELLIPSOMETRY

R. F. Steiger, J. M. Morabito, Jr., G. A. Somorjai and R. H. Muller

October 1968

A STUDY OF THE OPTICAL PROPERTIES AND OF THE PHYSICAL ADSORPTION OF GASES ON SILVER SINGLE CRYSTAL SURFACES BY LOW ENERGY ELECTRON DIFFRACTION AND ELLIPSOMETRY

R. E. Steiger,* J. M. Morabito, Jr.,** G. A. Somorjai and R. H. Muller

Inorganic Materials Research Division, Lawrence Radiation Laboratory,
Department of Chemistry and Chemical Engineering,
University of California, Berkeley, California

ABSTRACT

The physical adsorption of Kr, Xe, O_2, CH_4, C_2H_2, C_2H_4, n-C_4H_{10} on the (110) and (100) faces of silver single crystals has been studied by low energy electron diffraction (LEED) and ellipsometry in the temperature range from -195°C to 0°C and pressure range 10^{-10} to 10^{-6} torr. Adsorption isotherms in terms of optical thickness have been measured and from these data, heats of adsorption, the cross sectional areas of the adsorbed molecules and coverage ratios have been derived. LEED measurements indicate that the adsorbed phase is disordered on the silver surface. Ellipsometry is sensitive to the presence of the adsorbed gases in fractional monolayer coverages, while the LEED diffraction patterns were rather insensitive to this disordered adsorption below and up to the monolayer in the beam voltage range 50 to 150 eV.

---

*Present address: CIBA Photochemical Ltd., Fribourg, Switzerland

**Visiting scientist to Philips Research Laboratories, Eindhoven, The Netherlands

I. INTRODUCTION

There has been little work on the physical adsorption of gases on clean single crystal metal surfaces. However, it is now possible to obtain a clearer understanding of physical adsorption, i.e. its dependence on surface structure, the degree of ordering in the adsorbed phase, adsorption energetics, etc. with techniques such as field-emission- and field-ion-microscopy,[1-4] microbalance,[5] low energy electron diffraction[6] (LEED), ellipsometry[7] and others. Vacuum microbalance techniques are sufficiently sensitive only at pressures where contamination effects are appreciable. The limitations of the field ion microscope have been discussed by Brenner.[8] Neither field ion- nor field emission microscopy can be used to obtain accurate measurements of heats of adsorption or adsorption isotherms on clean single crystal surfaces. However, both ellipsometry[9,10] and low energy electron diffraction[11-13] techniques which have recently become available, can be used to monitor gas adsorption on single crystal surfaces and are reported[11-14] to be sensitive to the presence of adsorbed gas layers. In addition, by monitoring changes in the diffraction patterns, LEED has been used to study the degree of ordering in the adsorbed phase and appearance of surface structures as a function of coverage. It is for this reason that we have combined LEED and ellipsometry to study the physical adsorption of several gases on (110) and (100) silver at low temperatures (0°C to -195°C) and pressures (10^{-10} to 10^{-6} torr). Mass spectroscopy has been used to determine the composition of the ambient during the measurements. Ellipsometry has been used

to study the optical properties of the clean silver surface and their variation as a function of temperature. In addition, ellipsometry could not only detect the presence and amount of an adsorbed gas below the monolayer, but could also determine when a monolayer is completed on the clean single crystal surface. Isotherms (film thickness versus pressure) could be measured by ellipsometry and heats of adsorption, the cross sectional areas of the adsorbed gases and coverage ratios have been calculated from these measurements.

II. EXPERIMENTAL

A. Low Energy Electron Diffraction Apparatus

A modified Varian LEED apparatus using the post acceleration technique has been used for our measurements. The intensity of the individual diffraction spots has been monitored with a spot photometer.* The partial pressure of the gases, introduced into the LEED chamber by means of a Granville-Philips variable leak valve, has been measured with a hot filament ionization gauge (Varian Type UHV-14, calibrated for nitrogen). No correction has been applied for the different gases used, or for the difference (due to pressure gradients in the LEED diffraction chamber) between the recorded pressure and the one existing at the specimen. Although the measured pressures may be erroneous by as much as a factor of 10, this does not influence the shape of the adsorption isotherms, which were derived from relative measurements, to a noticeable extent because of the linear dependence[15] between pressure and ion current within the pressure range used.

A low temperature crystal manipulator[16] which allowed for easy movements in all directions (necessary for optical adjustments) and for good visibility of the fluorescent screen has been designed. The crystal temperature has been held constant to ±1°C (measured with a calibrated chromel-alumel thermocouple) by means of a cryostat (Type LAUDA, liquid circulation with methanol) or by a controlled flow of liquid nitrogen. Heating to maximum 600°C was possible by electrical heating of the crystal holder.

---

* Model 2000 Telephotometer, Gamma Scientific Instruments

B. Ellipsometry

An isotropic and absorbing medium can be described by two characteristic constants: refractive index n and absorption index κ, which can be determined experimentally by ellipsometry which is a measurement of the change in polarization upon reflection. These two optical constants have been derived from ellipsometer measurements performed at the lowest pressure obtainable. By resolving the electric vector of the incident polarized light into two components E_p and E_s (parallel and perpendicular to the plane of incidence, see Fig. 1), the state of polarization can be defined by the phase difference Δ between the parallel and perpendicular components upon reflection

$$\Delta = \delta_p - \delta_s \tag{1}$$

and the amplitude ratio tan ψ

$$\tan \psi = \frac{E''_s / E''_p}{E_s / E_p} \tag{2}$$

where E" stands for the electric field amplitude of reflected wave.

Upon reflection, the two components of the electric vector are retarded in phase and reduced in amplitude to different extents which is characteristic of the optical properties of the reflecting surface. Since ψ and Δ can be measured accurately (with an error of $\pm 0.02^\circ$ in our case) by means of an ellipsometer, the optical properties of the reflecting metal surface can be determined. If the metal is covered with a surface layer, the reflection formulae have to be modified and can be derived from Maxwell's equations. For the case of a thin, uniform,

non-absorbing and isotropic film on an absorbing substrate, this leads (as a first approximation) to a linear relationship between film thickness d and ψ and Δ

$$\Delta = \Delta - \alpha d \quad (3)$$

$$\psi = \bar{\psi} + \beta d \quad (4)$$

(where $\bar{\Delta}$ and $\bar{\psi}$ refer to the film free metal surface). α and β in equations (3) and (4) are constants which are functions of the optical constants of the pure metal surface, the refractive index of the film, the angle of incidence, the wavelength of the incident light and the refractive index of the incident medium (air). Values of ψ and Δ are calculated for different film thicknesses d by means of a computer program similar to the one described by McCracken,[17] and the measured film thickness d is determined by comparison of the computed with the experimental values. The equations used are based on the classical electromagnetic theory of continuous, isotropic media and plano parallel films of constant refractive index. Although it is not obvious that this model holds for film less than one monolayer thick, theoretical[18,19] and experimental[20-22] evidence have been presented in the literature that the film thickness thus derived is proportional to the amount of material adsorbed.

C. Ellipsometer

In order to avoid time consuming alignments caused by the need to remove the optical components from the LEED system each time the bakeout shroud is placed around the ultrahigh vacuum system, the optical components

of the ellipsometer* have been mounted on a movable table which can be rapidly placed over the frame of the LEED apparatus (Fig. 2). All our measurements have been obtained at $\lambda = 5461$Å using a fixed quarter wave compensator producing elliptically polarized incident light. Due to the geometry of the LEED diffraction chamber, an angle of incidence of 45° had to be chosen, although computations show (Fig. 3) that the relative phase shift Δ upon adsorption would be approximately three times larger and thus the measurements would be more sensitive at an angle of incidence of 75°. The refractive index of the adsorbed phase has always been assumed to be that of the liquid at a temperature close to that of our measurements.

D. Gas Analysis

A quadrupole mass spectrometer** was connected to the diffraction chamber (see Fig. 2) and placed directly below the sample. The mass spectra allowed the characterization of residual gases present in the diffraction chamber ($p_{tot} > 10^{-10}$ torr) and the determination of the composition of the gases*** used in the adsorption studies. No gaseous impurities were present in concentrations greater than 1% of the gas flux during our adsorption measurements.

---

* Model L119, Gaertner Scientific Instruments, Chicago, Illinois.

** Type EAI, mass range 1-500, sensitivity ca. 10A/Torr, minimum partial pressure of residual gases measureable ca 10^{-13} torr.

*** All gases used were Matheson high purity (> 99.8%).

E. Crystal Preparation and Properties

Single crystal rods (3/8") of pure silver* have been oriented by x-ray diffraction to within 1° of the desired surface plane [(110), (100) etc.], sectioned by spark cutting, ground parallel to the surface plane and mechanically polished. A major difficulty in combining LEED and ellipsometry lies inthe preparation of a surface suitable for both LEED and optical measurements. The silver surface was chemically polished with a solution of 100 cc 0.2 M KCN and 2 cc 30% H_2O_2. Argon or xenon ion bombardment (in the range 130-340 eV), followed by annealing at 150°C to remove any crystal damage, has been used for the final surface treatment. The resulting surface was highly reflecting, and gave sharp diffraction patterns.

The quality of the silver surface used in our adsorption experiments has also been investigated by electron microscopy (See Fig. 4) and interference microphotography (Fig. 5). Chemical polishing resulted in a microstructure with an average depth of approximately 600-900 Å, and scratches which occured occasionally were ca. 2000Å deep. Furthermore, the investigated surface was slightly curved as shown in Fig. 5.

The (110) surface of silver is unstable and highly susceptible to thermal faceting.[23] This is particularly true in the presence of oxygen, but this orientation showed signs of faceting even at temperatures

---

* Ag 99.999% (Mat. Research Corp.), total impurity content: 11.16 ppm. Impurities as determined by mass spectroscopy: Cu 0.3 ppm, Cd < 1.0, Sn < 0.3, Au < 2.0, Ta < 1.0, Fe 0.8, Nd < 0.4, Pd < 0.4, C 1.24, O_2 0.07, N_2 0.2 ppm. Other impurities were present in amounts < 0.1 ppm.

> 140°C in ultra high vacuum. Figure 6 shows the extra diffraction features which are due to the exposure of additional crystal planes under more severe thermal heating (451°C). Therefore, in order to bring the (110) surface to the same reproducible state, to preserve the crystal orientation and maintain optimum surface order, the following procedure was adopted; the crystal was heated to no higher than 85°C and cooled in the presence of the gas to be used in the adsorption study. The LEED diffraction pattern was also checked prior to a series of measurements as a precaution against any gross contamination. However, the diffraction pattern was fairly insensitive to the presence of adsorbed amorphous contaminants present in amounts less than a monolayer. Only oxygen formed an ordered structure on silver (110) at temperatures higher than 25°C as previously observed by Müller[24] and Pritchard and Jeanes[25] on thin films of evaporated silver.

III. CONTAMINATION PROBLEMS

Lander[6] has shown that contamination from the residual gases present in the ultra high vacuum can be a serious problem at low temperatures. The curves in Fig. 7, calculated on the basis of the kinetic theory of gases, show that the crystal surface could be covered with a monolayer within a relatively short period of time even at very low pressures. This was also confirmed by ellipsometer measurements which indicated a rapid contamination (most likely by water vapor) of the silver surface. Figure 8 shows the variation of the optical thickness with the time at -195°C (calculated for water). It is apparent from this curve that at this low temperature, the silver surface becomes contaminated almost immediately to an appreciable extent. The differences between calculated and measured contamination time (see Figs. 7,8) is most probably due to the uncertainty on our pressure measurements (see Section IIA). That the contamination is most probably due to water vapor has been shown by mass spectroscopy. Figure 8b illustrates the intensity variation of mass peak 18 (water) with temperature while the contamination curve of Fig. 8a was recorded ellipsometrically. The decrease in intensity of the zero order diffraction spot with time at -195°C (Figs. 9a,9b) shows that the rapid contamination of the silver surface can also be observed with LEED. The initial increase of the spot intensity with a change in temperature from +26°C to -195°C is due to a strong Debye-Waller effect (see Fig. 9b). A large broadening of the diffraction spots upon coverage of the surface with water (see Fig. 10) has also been observed. This may be due to a deflection of electrons by an electric field parallel to the crystal surface. This deflection may originate from domains of oriented surface dipoles (water)

as suggested by Müller and Chang[26] who observed a similar effect on freshly cleaved mica crystals.

Figure 11 also shows that the buildup of an adsorbed gas layer is slower if the crystal temperature is -40°C. The fact that this curve presents an inflection point after about 15 minutes may be explained by a nucleation phenomenon. Such inflection points have been observed in almost all cases which may indicate that the contamination becomes appreciable after a stable nucleus of a critical size has formed.

It has been possible to keep the metal surface free of contamination* in our adsorption measurements during the time necessary for ellipsometer measurements (5 to 20 min.) down to a temperature of -72°C. Therefore, all our measurements were performed in the temperature range -72 to -10°C. Furthermore, all adsorption studies were carried out using a steady flux of gas in order to maintain the purity of the gas even at low pressures ($> 10^{-10}$ torr). Both the continuous flux and the low pressure of the gas minimized the possibility of back streaming which was mostly due to CO, argon, and H_2 from the Vac-Ion** pump as shown by mass spectroscopy.

Typical results of the phase shift Δ versus time for krypton at various pressures are shown in Fig. 12. The contamination at $p = 10^{-10}$ torr is more appreciable due to the greater percentage of the residual gases at low pressures compared to higher pressures ($>10^{-10}$ torr) where the percentage of residual gases is lower.

---

* The resolution of our optical thickness measurements is 0.3-0.5Å.

** Ultek Corporation

IV. ELLIPSOMETRY RESULTS

The optical constants n and κ, measured on the (110) surface of silver, are shown in Fig. 13 as a function of temperature at two different wavelengths. Similar measurements on the (100) face indicated that the temperature dependence of the optical constants is similar to that of (110) face of silver. These curves have been corrected for birefringence effects due to anisotropies in the LEED windows.* [Correction: $d\bar{\psi}$ = 0.00, $d\bar{\Delta}$ = 4.92°, equally applied to all measured values of $\bar{\Delta}$]. This correction has been applied after comparison of the optical constants of a standard surface measured successively when this surface was placed into the LEED diffraction chamber at atmospheric pressure, reduced pressure (10^{-8} torr) and outside the LEED chamber. As a standard surface, we used the hypothenuse of a right angle prism which had been covered with a thin layer of aluminum (by metal evaporation) and protected against alteration and contamination by a thin layer of silicon monoxide. Periodical measurements of this surface showed that its optical constants did not change to an appreciable extent over a period of several months, (change in Δ: 0.04°). Removal of the windows showed that the birefringence of the windows was due to mechanical strain which occurred primarily in the front window. No error has been introduced by the presence of a metallic grid between crystal and front window of the diffraction chamber. All measurements of $\bar{\psi}$ and $\bar{\Delta}$ have been obtained in four zones as described by

---

*Selected 7056 glass of 3/8" thickness, flat to 5 wavelengths and parallel to 1 minute of arc over a 3/4' diameter circle in the center has been sealed to the 8" and 6" flanges of the LEED diffraction chamber.

McCracken et al.[27] and an average value was used for the computation of the optical constants of the pure metal surface.

Adsorption measurements in the pressure range 10^{-10} to 10^{-6} torr have shown that ellipsometry is sensitive to less than 10^{-8} gcm^{-2} of adsorbed gas. Therefore, from the measurement of the phase shift Δ between the two component waves at different pressures (as shown for krypton in Fig. 14a), optical thicknesses could be calculated and adsorption isotherms plotted (see Fig. 14b). That these measurements are relative to the clean silver surface follows from Eq. (3) where $\bar{\Delta}$ is the measured phase shift for the clean surface at temperature T and residual pressure p_o (in order of 10^{-10} torr) recorded before admission of the gas. Δ is the measured phase shift at temperature T and pressure p_1 of the gas. The curves in Fig. 15 show also that our optical thickness calculations are still valid even if the measured relative phase base for the silver surface are erroneous by as much as 7 degrees. Errors introduced by birefringence effects due to the LEED windows do therefore not affect the values of our optical thicknesses beyond the error limit of 0.3 to 0.5 Å.

Measurements on the (100) surface of silver indicated that the form of the isotherms is similar to those obtained on the (110) surface. This

has been confirmed for the adsorption of krypton, acetylene and xenon, and indicated that the magnitude of the heats of adsorption is the same on these two faces of silver, as was also observed by Rhodin on different crystal faces of copper.[5]

Adsorption isotherms have also been calculated from the measured values of Δ versus pressure for oxygen, xenon, methane, ethylene, acetylene and n-butane and are similar in shape (Type I, Langmuir) to those shown in Fig. 14b for krypton. From the temperature dependence of the obtained adsorption isotherms, $\log_{10} p$ vs. $1/T$ can be plotted (as shown for krypton in Fig. 16a), and isosteric heats of adsorption (ΔH_{st}) calculated at each coverage from the slope of these curves (see Figs. 16a, 16b, and 17).

A. Discussion of Ellipsometry Results

1. Optical constants of the pure silver surface

As mentioned previously (see Section IID), the (110) surface of silver is highly susceptible to thermal faceting. Direct evidence of faceting could only be obtained by a change in the LEED diffraction pattern which occurred when the crystal was heated to above 300°C in ultrahigh vacuum (see Fig. 6). Ellipsometer measurements, however, showed that the crystal surface was altered when heated to only 140°C in ultrahigh vacuum, that is, the relative phase was approximately 0.3° more positive than in the case of normal surface treatment (heating to 85°C) In agreement with this result, we also noticed thermal instability of the silver (110) surface when Debye-Waller measurements[28] were initiated at higher temperatures (> 140°C) instead of 85°C. In order to explain the ellipsometry results, the overheated surface has been considered theoretically as a pure silver surface (having the optical constants indicated

in Fig. 13) covered with a transitional layer characterized by different fractions f of the metal optical constants (see Fig. 18). These curves show that the relative phase Δ becomes more positive if the optical constants of the transitional layer lie between those of the pure metal and those of vacuum. The optical film thickness of this layer is in the Angstrom-range for a change in relative phase of the order of + 0.3 degrees as measured ellipsometrically, which suggests that the overheated silver (110) surface behaves like a dislocated roughened surface (on an atomic scale). This interpretation agrees with the fact that no sign of classical thermal faceting[29] could be observed within the resolution of the electron microscope replica (approximately 150Å).

The accurate measurement of metal optical constants is of considerable importance in the calculation of energy bands and the evaluation of inter-band transition and free electron effects.[30] Our measurements of the optical constants of the pure silver (110) surface have been obtained under conditions of minimum surface contamination. Although we have no information on the influence of the surface roughness on the measured optical constants, the large scattering between the previously published[31] optical constants of silver surfaces suggests that these constants may be strongly dependent on the quality of the surface. Our values (Fig. 13) lie between those obtained previously[32] on thick, annealed and aged silver films ($n = 0.055$, $n\kappa = 3.32$) and those for thin films of evaporated silver[31] ($n = 0.17$, $n\kappa = 2.94$).

The principal uncertainty in the measured constants may be due to birefringence effects in the cell windows. Additional errors are probably caused by the thermal instability of the silver (110) surface above 140°C and the rapid contamination of the bare surface below -100°C.

2. Heats of adsorption for Xe, Kr, O_2, C_2H_2, C_2H_4 and CH_4

The gas-surface interaction is closely related to the heat of adsorption at zero coverage ($\theta = 0$). These heats, which have been calculated by assuming linear extrapolation to $\theta = 0$, are summarized in Table I for the gases studied, together with the polarizabilities (parallel to the sigma bond for ethylene and acetylene) and the heats of condensation. The latter marks the upper limit to the lateral (gas-gas) interaction energy. The initial heat of adsorption may in reality start at higher values, decrease in the very low film thickness range (≤ 1 Å), and then begin to increase as observed previously by Aston.[33] However, we could not calculate accurate heats for coverages below 1Å from our experiments. Nevertheless, it can be seen from Table I that the energies of the gas-surface and the gas-gas interaction are of the same order of magnitude on the (110) surface of silver (with the exception of xenon). The fact that the initial heat of adsorption for xenon is considerably greater than that of krypton may be related to the large difference in the polarizabilities and the atomic diameters of these gases. As a comparison, we list the initial heats of adsorption for xenon on tungsten (9-10 kcal/mole) and for krypton on tungsten (4.5 - 5.9 kcal/mole), as reported by both Gomer[4] and Ehrlich[1,34] using field-ion and field emission microscopy. Furthermore, the magnitude of the initial heats of adsorption for the gases studied (see Table I) indicates that the forces involved are of the van der Waals type.

The variation in the isosteric heat of adsorption which, at any coverage θ, corresponds to the sum of the potential and kinetic energy changes (due to the adsorption process) of the gas, depends on the cooperative effects between these energy terms. The gas-metal interaction decreases with surface coverage while the gas-gas interaction increases. It can be seen from Figs. 16b, 17 that for silver (110), the absolute change in the gas-gas interaction with coverage is greater than the absolute change in the gas-metal interaction.* Rhodin,[5] using the microbalance technique, also observed an increase in the isosteric heats of adsorption with coverage for nitrogen on single crystal copper surfaces and for argon on zinc at low temperatures. He observed a maximum in the heat curve at monolayer coverage followed by a sharp decrease, but our measurements did not allow accurate heat calculations at higher coverage as measurements close to the vapor pressure of the gas at the temperature of the experiment $p > 1$ atm. for all the gases studied would be required. The heat of adsorption should approach the heat of condensation (indicated on the graphs in Figs. 16b, 17) as the partial pressure of the gas approaches the equilibrium vapor pressure and as the thickness of the adsorbed layer increases. It can be expected then that a physically adsorbed layer of gas several molecular diameters thick behaves like a liquid. Gomer[35] has presented evidence for this fact using field ion microscopy.

* The rather high gas-gas interaction for acetylene may be fictitious as our calculations have been based on two temperatures only.

3. Comparison of optical thickness and molecular dimensions

The adsorbed phase has been considered as a non absorbing, three dimensional liquid characterized by a constant index of refraction (the validity of this assumption has been discussed in Section IIB.). The optical thickness of the adsorbed layer at monolayer coverage measured by ellipsometry (which corresponds to the flat, constant portion of the adsorption isotherms) can be compared to an effective molecular diameter in the liquid state (d_o) as obtained from

$$d_o = \frac{M}{\rho N_A}^{1/3} \qquad (5)$$

where M is the molecular weight and ρ the density of the liquid at the temperature of measurement (see Appendix), N_A is Avogadro's number. The calculated and the measured thicknesses are listed in Table II, columns 3 and 4, and show good agreement which supports the use of the classical theory for monolayer films. No agreement would be observed in using either gas densities for the calculation of d_o, or the refraction index of the gas in the calculation of optical thicknesses. The difference between the calculated and measured values for n-butane may be due to the orientation of the n-butane molecule on the silver surface. Similar agreement between ellipsometrically measured thickness at monolayer coverage and the dimensions of the adsorbed molecules has been obtained by Archer[36] on etched surfaces of silicon with several gases adsorbed (H_2O, CCl_4, acetone).

The measured thickness of the adsorbed layer, d, can also be converted to a surface concentration of atoms or molecules by the formula,

$$\text{atom/cm}^2 = \frac{\rho d \, N_A}{M} \qquad (6)$$

and compared to the number of silver atoms on the ideal (110) surface which is reported to be 8.5×10^{14}.[37] The ratio of these two numbers (coverage ratio) indicates the number of silver atoms covered by each atom or molecule of the adsorbed gas. Table II, column 6, shows that ethylene, krypton, xenon and oxygen cover roughly two silver atoms, while n-butane covers 4 silver atoms when adsorbed under our experimental conditions.

Effective areas of coverage for adsorbed molecules can be calculated under the same assumption as that used in the calculation of the surface concentration. Experimentally, cross sectional areas are generally measured by adjusting the surface areas as determined with other gases until they yield the same value as nitrogen which is assumed to give the most accurate surface areas. However, McClellan and Harnsberger[38] have recently concluded that the size of the adsorbed molecule depends not only on the nature of the adsorbent, but on the temperature and the reference substance also.

The optical thickness at monolayer coverage has been determined from the adsorption isotherms which appeared to be of Type I. (Langmuir see Fig. 19.) The thickness could then be converted into a molecular area by taking the reciprocal value of Eq. 6. In Column 7, Table II we compare our experimental results with those reported in the literature for metal substrates. When values were available on several metals, an average was taken (Column 8).

The relatively good agreement between these values shows that ellipsometry provides an independent measurement of cross sectional areas without depending on an internal standard such as nitrogen.

V. LLED ANALYSIS OF PHYSICAL ADSORPTION

A. Results

The absence of extra features in the diffraction patterns recorded during our physical adsorption measurements indicates that the adsorbed phase is disordered on silver in the temperature range (0°C to -195°C) and pressure range (10^{-10} to 10^{-6} torr) studied. This lack of ordered structures could be explained by desorption or perturbation of the weakly bound array by the electron beam. However due to the small specimen area covered by the electron beam, desorption cannot be detected by mass spectroscopy as the gas pressures coming off the surface is negligible (10^{-13} torr). In agreement with our observations, Pritchard and Jeanes[25] did not observe any change in the LEED pattern when molecular oxygen at a pressure of 10^{-6} torr was adsorbed on the (110) plane of evaporated silver between 20°C and -100°C. A change in the work function by +150 mV indicated, however, that adsorption of oxygen on Ag (110) occurred.

Lander[5] reports that physically adsorbed xenon on graphite is ordered at -183°C and 10^{-3} torr, but no ordered phase has been observed under those conditions on silver. Only a gradual increase in the background intensity and a blurring of the normal diffraction features due to the disordered nature of the adsorbed xenon results in our experiments. Other ordered adsorption structures are reported by Lander for substances which should be classified as weakly chemisorbed rather than physically adsorbed.

Although ellipsometry indicated that gas adsorption close to a monolayer had taken place below 10^{-8} torr and 0°C, the background intensity increased and the (00)-diffraction spot intensity decreased to an appreciable extent only at

pressures higher than 10^{-7} torr and beam voltages of about 50 eV. Both the intensities of the background and the (00) spot returned to their original values when the gas was removed, which is in agreement with the small heats of adsorption (weak bonding) as measured by ellipsometry. These measurements also suggest that the adsorption is reversible under our experimental conditions (this could not be confirmed ellipsometrically because of the rapid contamination of the surface).

B. Discussion

All measurements were performed at beam voltages of 50 eV or more. Similar results may not be obtained when a Faraday cage is used for spot intensity measurements as this method may be a more sensitive measure of very small variations in spot intensities. Also, these intensity variations due to gas adsorption may be stronger at lower beam voltages ($\leq$ 10 eV) as suggested by Lander and McRae.[39] Nevertheless, our experiments showed that ellipsometry is more sensitive than LEED in the range $\geq$ 50 eV for the detection of disordered gas adsorption at coverages below and up to one monolayer, and that LEED is not a sufficient criterion to define surface cleanliness in this voltage range. The high sensitivity of ellipsometry in the submonolayer range should make this technique suitable for the calibration of the Auger secondary electron emission, the sensitivity of which is still uncertain for gaseous impurities adsorbed to less than a monolayer.

The magnitude of the measured heats of adsorption suggests that the adsorbed molecules are not bound to any particular surface atoms, but move freely over the surface of the metal. This occurs when the energy

required for motion is appreciably lower than the energy of desorption. However, at lower temperature (< -195°C) and higher pressures, ordering should occur due to the restriction in free motion, but refractive index measurements of adsorbed gases at liquid helium temperature on copper and gold single crystals by Kruger[40] indicated that a liquid-like state of the adsorbate persists. Nevertheless it would be interesting to extend our measurements to lower temperatures and higher pressures for the study of multilayer formation, two dimensional condensation and phase transformations in the adsorbed layer.

Finally, the fact that the LEED diffraction pattern remains characteristic of a clean surface even after adsorption to a monolayer seems to indicate that the gas is adsorbed in "patches" on the metal surface. The increase of the isosteric heat of adsorption at fairly low coverages also suggests that the adsorbed molecules or atoms readily associate.

VI. CONCLUSIONS

The combination of structure sensitive LEED and coverage sensitive ellipsometry has provided unique information on the adsorption of several gases on clean single crystal silver surfaces in the temperature range from 0°C to -195°C and at pressures between 10^{-6} and 10^{-10} torr. A LEED analysis of all the adsorption results on (110) and (100) silver indicated that the physically adsorbed phase is disordered under the pressure and temperature conditions of our experiments. This is not surprising due to the weak binding between the adsorbed phase and the silver surface as calculated from ellipsometer measurements. In cases of weak binding between the adsorbed phase and the metal, ordering can perhaps only occur at temperatures and pressures considerably below the triple point of the gas. The adsorbed gas is then more localized on the surface and may order. Ellipsometry was found to be sensitive to coverages below the monolayer and useful in determining when a monolayer forms on a single crystal surface. LEED was rather insensitive to this disordered adsorption at beam voltages $\geq$ 50 eV and is therefore not a sufficient criterion for surface cleanliness in this voltage range. LEED may be more sensitive to the presence of this disordered adsorption in the range 0 to 10 eV and measurements should be initiated in this range.

The fact that the LEED diffraction pattern remained characteristic of a clean surface even after the adsorption of a monolayer of gas seems to indicate that the gas atoms are adsorbed in "patches" on the silver surface.

Contamination from the residual gases present in the ultra high vacuum

($\approx 10^{-10}$ torr) was appreciable at temperatures below -100°C as indicated by ellipsometer measurements. The removal of such contamination is essential for the low temperature studies (below -100°C) of clean metal surfaces.

Both LEED and optical measurements confirmed the instability of the silver (110) surface. It seems that this instability and the physical quality of the surface are important considerations for optical measurements.

From the adsorption isotherms measured by ellipsometry, isosteric heats of adsorption and their variation with surface coverage, cross sectional areas of adsorbed molecules and coverage ratios (number of surface atoms covered by adsorbed molecules) have been determined. The calculated cross sectional areas were independent of any standard such as nitrogen. The magnitude of the heats of adsorption confirmed that the interaction between the studied gases and silver [both (100) and (110)] is primarily due to Van der Waals forces. The increase in the heat of adsorption with film thickness is due to the lateral interactions between the adsorbed molecules on the surface which increase more rapidly with coverage than the decrease in the gas-surface interactions. The fact that this increase occurs at low coverage indicates that the surface is relatively homogeneous in energy and that the adsorbed molecules have a tendency to associate (clustering). This further substantiates the possibility of a "patch-like" adsorption model.

Finally, the thickness of the adsorbed phase at the monolayer was found to be comparable to the diameter of the molecules in the liquid state. This suggests that the presence of cracks, flaws, etc., as indicated by

both electron and interference microscopy, does not significantly affect the optically determined film thickness.

This is the first attempt to study physical adsorption with both LEED and ellipsometry. The results obtained in this study of physical adsorption indicate that the combination of LEED and ellipsometry will provide interesting information on a large variety of other surface phenomena such as epitaxy, chemisorption and on the interpretation of LEED diffraction patterns.

Acknowledgements: This work was performed under the auspices of the United States Atomic Energy Commission.

REFERENCES

1. G. Ehrlich, Brit. J. Appl. Phys. 15, 349 (1964).
2. G. Ehrlich, Metal Surfaces (ASM, Metals Park, Ohio, 1962).
3. G. Ehrlich and F. G. Hudda, J. Chem. Phys. 33, 4 (1960).
4. R. Gomer, Disc. Faraday Soc. 28, 23 (1959).
5. T. N. Rhodin, Jr., J. Am. Chem. Soc. 72, 4343, 5691 (1950).
6. J. J. Lander and J. Morrison, Surface Sci. 6, 1 (1967).
7. G. A. Bootsma and F. Meyer, Surface Sci., to be published.
8. S. S. Brenner, Metal Surfaces (ASM, Metals Park, Ohio, 1962).
9. Ellipsometry in the Measurement of Surfaces and Thin Films, Symposium Proceedings, Washington 1963, National Bureau of Standards Misc. Publ. 256 (1964).
10. Proceedings of the Conference on Recent Developments in Ellipsometry, Nebraska, August 7-9, 1968, University of Nebraska press, to be published.
11. J. J. Lander, Prog. Solid State Chem. 2, 26 (1965).
12. J. W. May, Ind. Eng. Chem. 57, (7), 19 (1965).
13. J. M. Morabito, Jr., and G. A. Somorjai, J. Metals 20, 5 (1968).
14. R. J. Archer and G. W. Gobeli, J. Phys. Chem. Soc. 76, 343 (1965).
15. S. Dushman, Scientific Foundations of Vacuum Technique, (John Wiley and Sons, Inc., New York, 1962).
16. E. I. Kozak and J. M. Morabito, Jr., UCRL Report 18038, University of California, Berkeley, Lawrence Radiation Laboratory, (1968); to be published.
17. F. L. McCracken, J. P. Colson, United States Department of Commerce, National Bureau of Standards, Technical Note 242.

18. C. S. Strachan, Proc. Cambridge Phil. Soc. 29, 116 (1933).

19. D. V. Sivukhin, Zhurn. Eksper. Theor. Fiz. S.S.R. 18, 976 (1948); 21, 367 (1951).

20. T. Smith, J. Opt. Soc. Am. (1968); to be published.

21. L. S. Bartell, J. F. Betts, J. Phys. Chem. 64, 1075 (1960).

22. J. R. Miller, J.E. Berger, J. Phys. Chem. 70, 3070 (1966).

23. A. J. Moore, Metal Surfaces (ASM, Metals Park, Ohio, 1962).

24. K. Müller, Z. Physik, 195, (2), 105-124 (1966).

25. J. Pritchard and M. R. Jeanes, private communication.

26. K. Müller and C. C. Chang, Surface Sci. 9, 455 (1968).

27. F. L. McCracken and J. P. Colson, J. Res. Nat. Bur. Stand. 67A, 363 (1963).

28. J. M. Morabito, Jr., R. E. Steiger and G. A. Somorjai, to be published.

29. E. D. Hondros and A. J. Moore, Acta Met. 7, 521 (1959).

30. H. Ehrenreich and H. R. Philipp, Phys. Rev. 128, 1622 (1962).

31. Landolt-Bornstein, Phys. Chem. Tabellen.

32. L. G. Schulz and F. R. Tangherlini, J. Opt. Soc. Am. 44, 357 (1962).

33. J. G. Aston and H. Chon, J. Phys. Chem. 63, 1015 (1961).

34. G. Ehrlich and G. F. Hudda, J. Chem. Phys. 30, 493 (1959).

35. R. Gomer, J. Phys. Chem. 63, 468 (1959).

36. R. J. Archer, Ellipsometry in the Measurement of Surfaces and Thin Films, Symposium Proceedings, Washington, 1963.

37. J. Bénard , J. Oudar, and F. Cabané-Brouty, Surface Sci. 3, 359 (1965).

38. M. L. McClellan and H. F. Harnsberger, J. Coll. Interf. Sci. 23, 577 (1967).

39. J. J. Lander and E. G. McRae, private communication.

40. J. Kruger and W. J. Ambs, J. Opt. Soc. Am. 49, 1195 (1959).

41. J. Hildebrand and R. L. Scott, The Solubility of Nonelectrolytes, Dover Publications, New York, 1964.

Table I

gas adsorbed	ΔH_{st} (θ=0) (kcal/mole)	$\alpha \times 10^{24}$ (cm^3)	$\Delta H_{cond.}$ (kcal/mole)
Kr	1.4	2.46	2.31
Xe	6.1	4.00	3.02
O_2	1.8	3.88 (O^{2-})	1.63
CH_4	1.0	2.60	1.96
C_2H_2	1.0	2.43	4.27
C_2H_4	1.6	3.59	3.24

TABLE II.

1	2	3	4	5	6	7	8
gas adsorbed	surface temperature < °C >	d_o calc. < Å >	d_o measured < Å >	Molec./cm^2 x 10^{14}	Coverage ratio Ag : gas	Cross Section meas. < Å^2/molec. >	Cross Section Lit < Å^2/molec.>
Kr	- 68	5.4	6.0	3.9	2.2:1	25.6	21.5 at -183°C, -196°C
Xe	- 72	4.3	4.0	5.1	1.7:1	19.6	22.5 at -183°C, -196°C
O_2	- 72	5.0	4.7	3.8	2.2:1	26*	17.4 at -183°C, -196°C
C_2H_2	- 72	4.1	3.8	5.4	1.6:1	18.3	22.0 at 78°C
n-C_4H_{10}	- 42	5.3	3.6	2.4	3.5:1	42	43.4 at -78°C

*Calculated from density at $T_{crit.}$ = -118.8°C.

FIGURE CAPTIONS

Fig. 1 Schematic of incident (E) elliptically polarized and reflected (E") plane polarized light with electric field components parallel (subscript p) and normal (subscript s) to the plane of incidence. Δ-phase difference between the two components in incident light, chosen to be eliminated by reflection.

Fig. 2 Combination of LEED and ellipsometer.

A. He-Ne

B. Light chopper

C. Polarized circle

D. Compensator circle

E. LEED chamber

F. Analyzer circle

G. Photomultiplier

H. Camera

I. Low temperature crystal manipulator

K. Liquid nitrogen cold trap

L. Cryostat

M. Quadrupole mass spectrometer

N. Mobile table

Fig. 3 Sensitivity of relative phase Δ and amplitude ψ for film thickness d on silver as a function of angle of incidence (film refractive index 1.35, optical constants of the substrate: $n_c = 0.14 \quad [1 + 34i]$).

Fig. 4 Electron micrograph of a carbon replica of a chemically polished silver (110) surface. Maximum depth of pits 600Å.

Fig. 5 Interference micrograph of a chemically polished (110) silver surface. Thallium light, λ = 5350Å.

Fig. 6 LEED diffraction pattern of the faceted (110) surface of a silver single crystal as obtained after heating to 451°C during 12 hours in a vacuum of $2X10^{-9}$ torr (energy of the incident electron beam: 105 eV).

Fig. 7 Contamination time for monolayer formation as a function of the gas pressure, calculated for sticking coefficient of unity.

Fig. 8a Measured contamination curve on silver (110) at -195°C and $4X10^{-10}$ torr. Fig. 8b. (Insert) Variation of mass peak 18 for the ambient during build up of the contaminant layer.

Fig. 9(a) The intensity of the specular reflection vs. beam voltage during formation of water layer on silver (110) as recorded as a function of contamination time, ($4X10^{-10}$ torr). Fig. 9b Variation of the intensity of the specular reflection for 94 eV electrons as a function of time.

Fig. 10 LEED diffraction pattern of the (110) surface of a silver single crystal covered with a 19Å thick layer of water (energy of the incident electron beam: 125 eV).

Fig. 11 Contamination in ultrahigh vacuum at -195°C and -40°C (assuming a refractive index of 1.25 for the calculation of the optical thickness d).

Fig. 12 Measured phase shift Δ versus time for the adsorption of krypton on the (110) face of silver at -54°C. Partial pressures of krypton: a) 6.6×10^{-9} torr, b) 1.2×10^{-9} torr, c) 1.0×10^{-10} torr.

Fig. 13 Optical constants $n_c = n(1 + i\kappa)$ for silver (110) as a functional temperature at wavelengths of 5461Å and 5893Å.

Fig. 14 Relative phase, Δ, and optical thickness versus pressure for krypton at various temperatures as obtained on the (110) surface (closed circles) and the (100) surface of a silver single crystal. [(100) data shifted to account for differing substrate properties.] Insert: Adsorption isotherm calculated from measured phase shift.

Fig. 15 Effect of a 7° error in absolute value of Δ on measured film thickness as calculated for n-butane on Ag (110). (n = 1.3)

Fig. 16 (a) Log p versus 1/T plot for krypton. (b) Isosteric heats of adsorption versus optical thickness for krypton and xenon. d_{Xe} and d_{Kr} correspond to the measured thickness of the monolayer, $\Delta H_{cond.}$ = heats of condensation.[41]

Fig. 17 Isosteric heats of adsorption versus optical thickness as calculated from the adsorption isotherms for oxygen, methane, ethylene, and acetylene.

Fig. 18 Surface roughness of silver treated as transitional layer with indicated fraction, f, of metal optical constants calculated by the following formula:

$$n = n_{substra.} + (1-f)(1-n_{substra.})$$

$$\kappa = (f\,\kappa_{substra.})$$

Fig. 19 Optical thickness d versus partial pressure of acetylene at $T = 60°C$ and $-72°C$ on Ag (110).

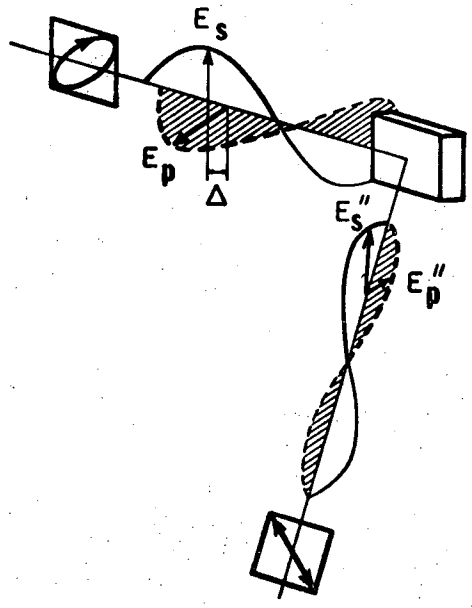

Fig. 1

XBL686-2859

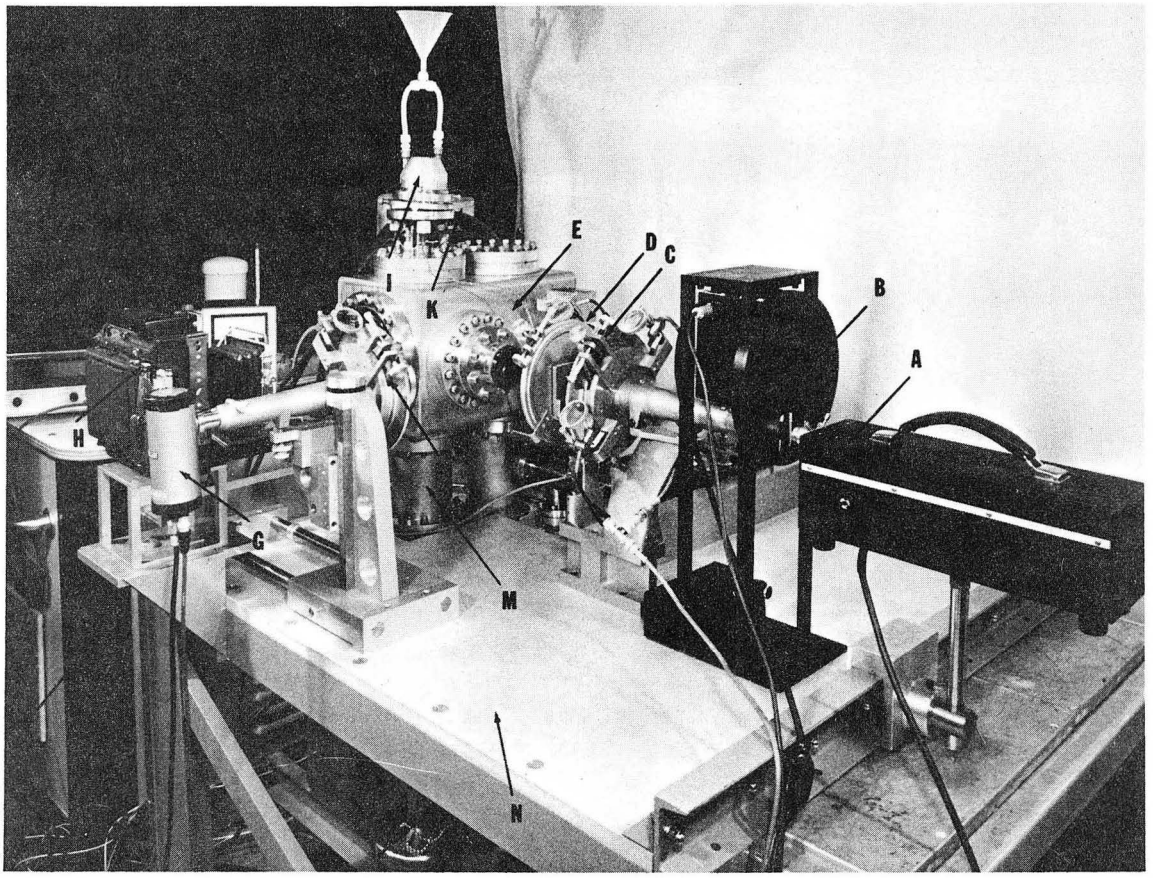

XBB 686-3329-A

Fig. 2

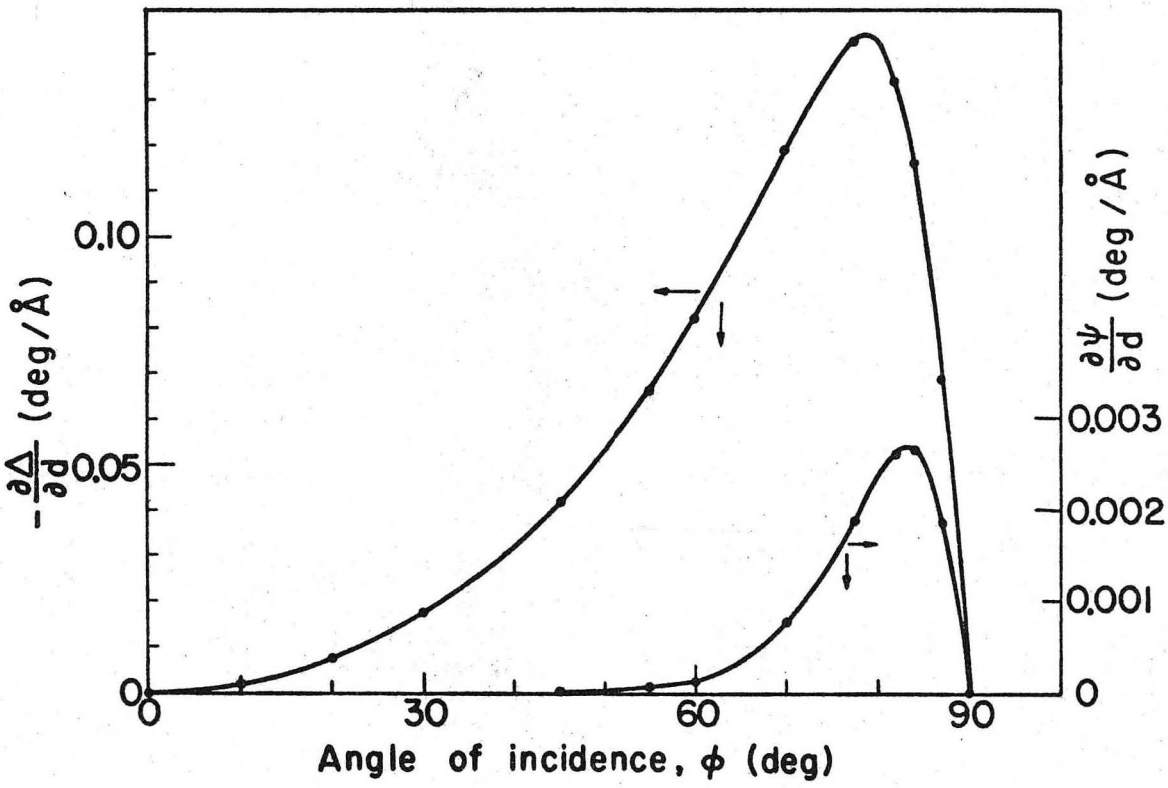

XBL 687-3398-A

Fig. 3

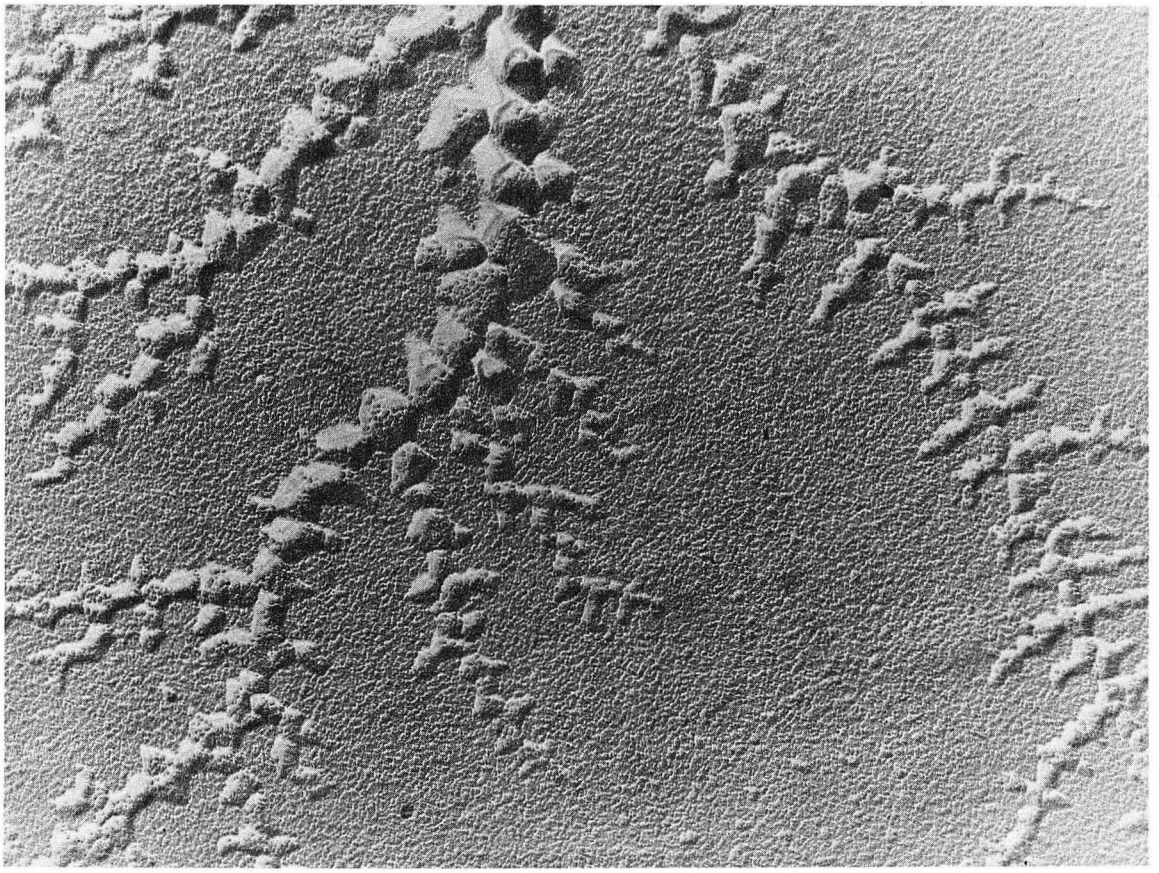

XBB 6811-7094

Fig. 4

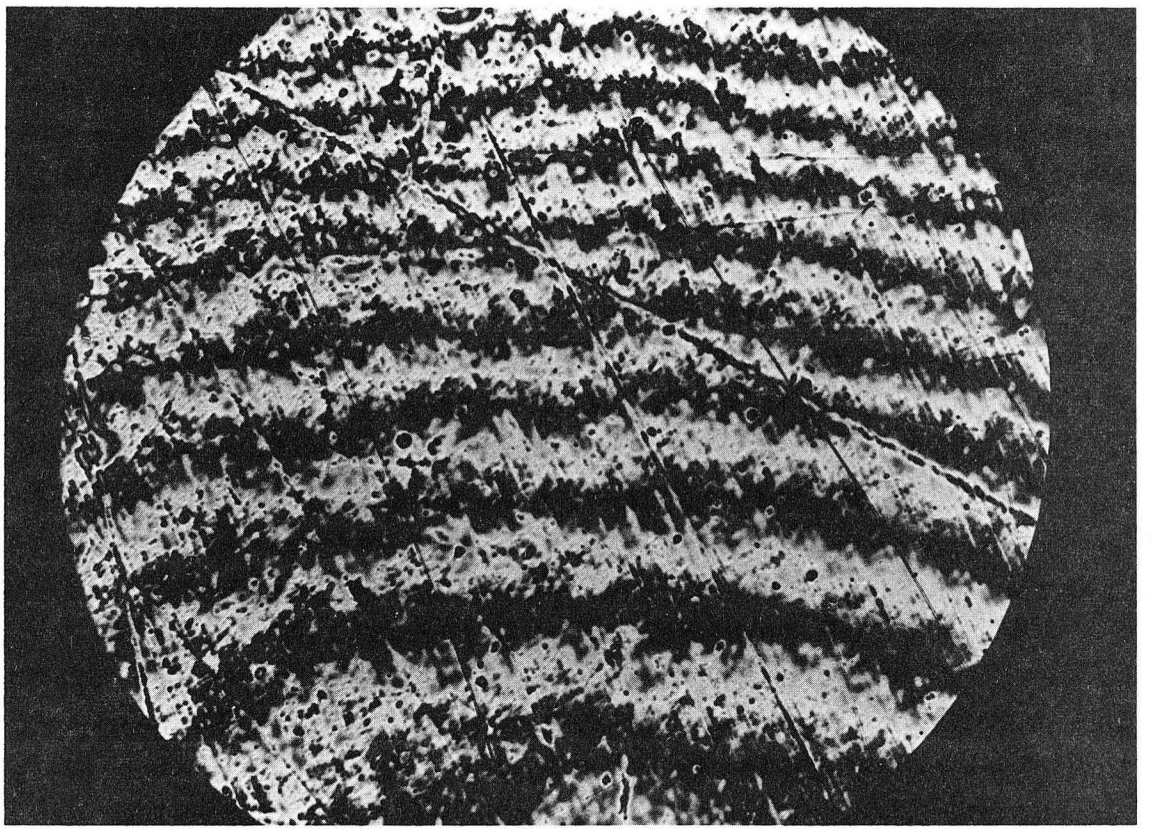

XBB 6811-7095

Fig. 5

XBB 688-4999

Fig. 6

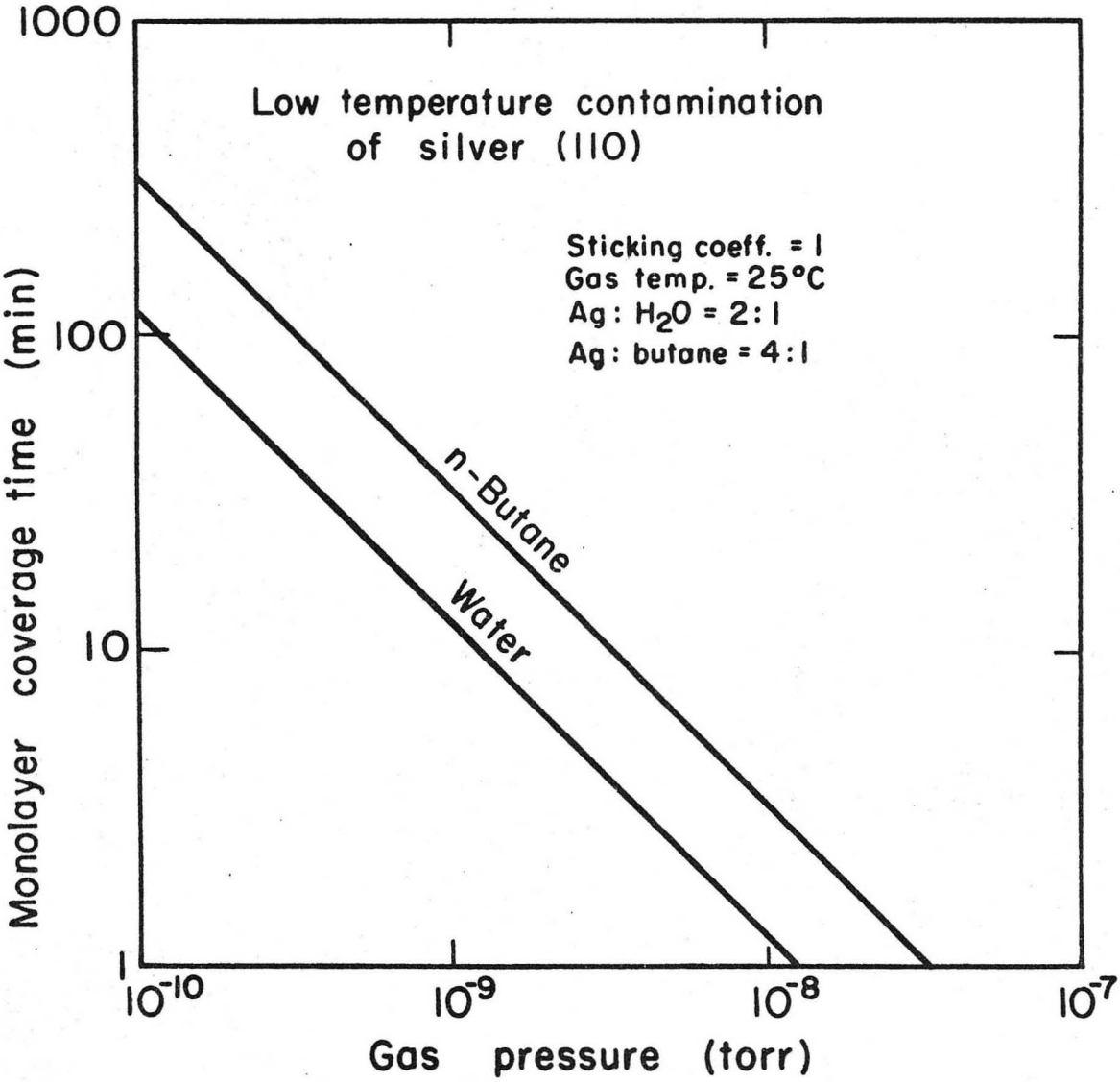

XBL687-3171

Fig. 7

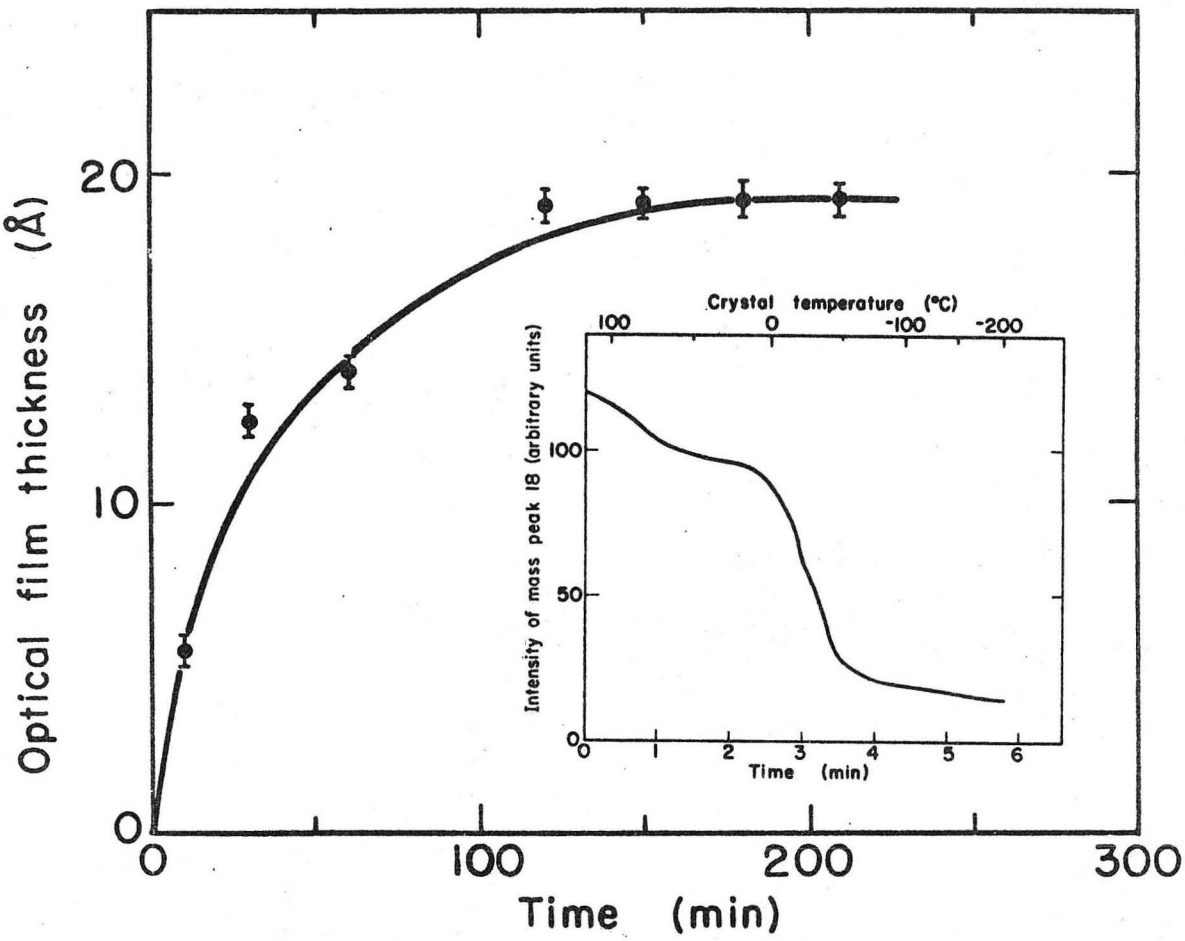

XBL 687-3172-A

Fig. 8a,b

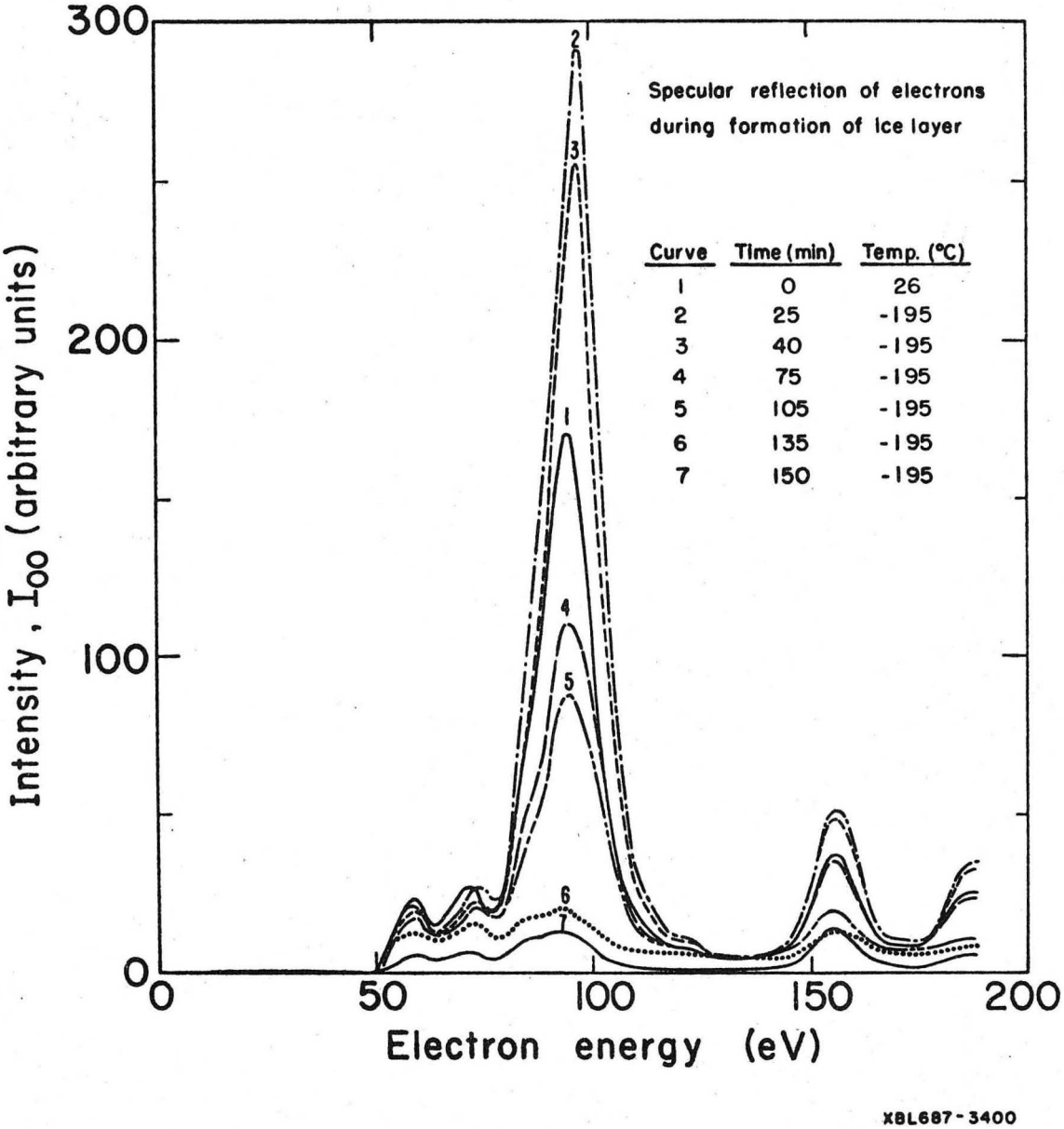
Specular reflection of electrons
during formation of ice layer
Curve Time (min) Temp. (°C)
1 0 26
2 25 -195
3 40 -195
4 75 -195
5 105 -195
6 135 -195
7 150 -195
Intensity, I_{00} (arbitrary units)
Electron energy (eV)
0
100
200
300
0
50
100
150
200
1
2
3
4
5
6
7
XBL687-3400

Fig. 9a

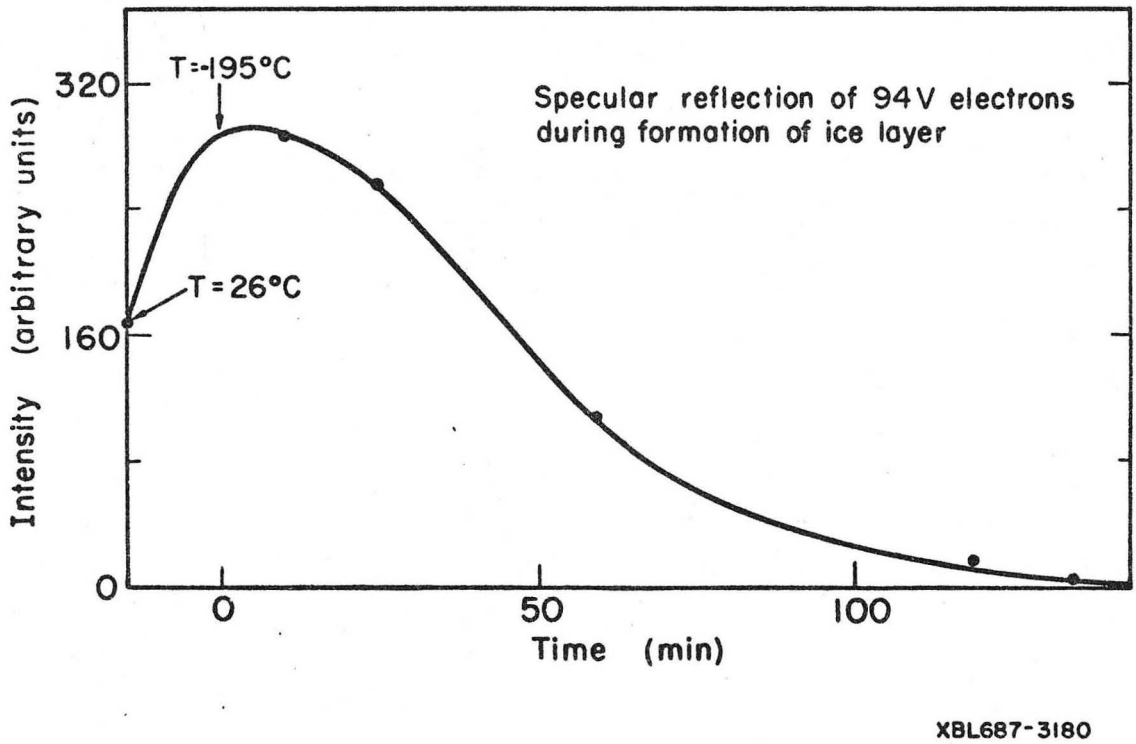
T=-195°C
T=26°C
Specular reflection of 94V electrons
during formation of ice layer
320
160
0
Intensity (arbitrary units)
0
50
100
Time (min)
XBL687-3180

Fig. 9b

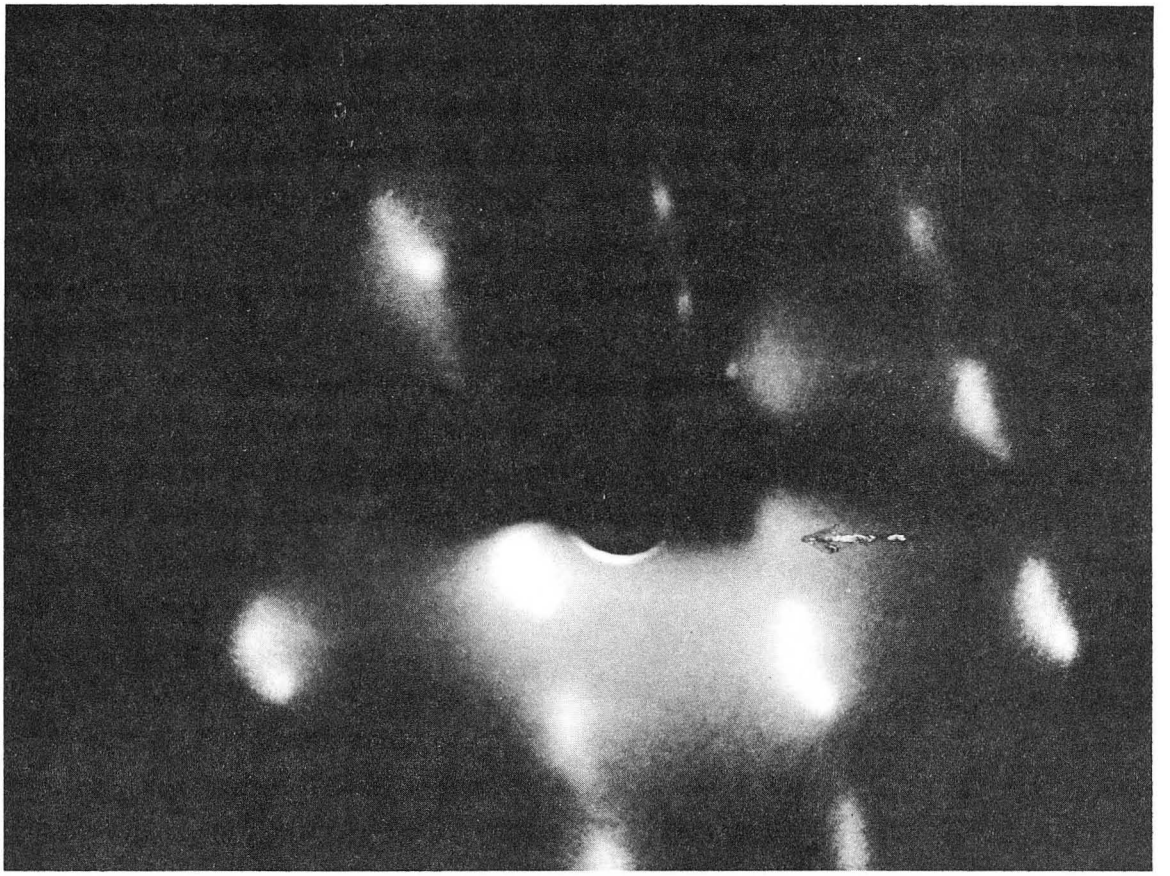

XBB 688-4998

Fig. 10

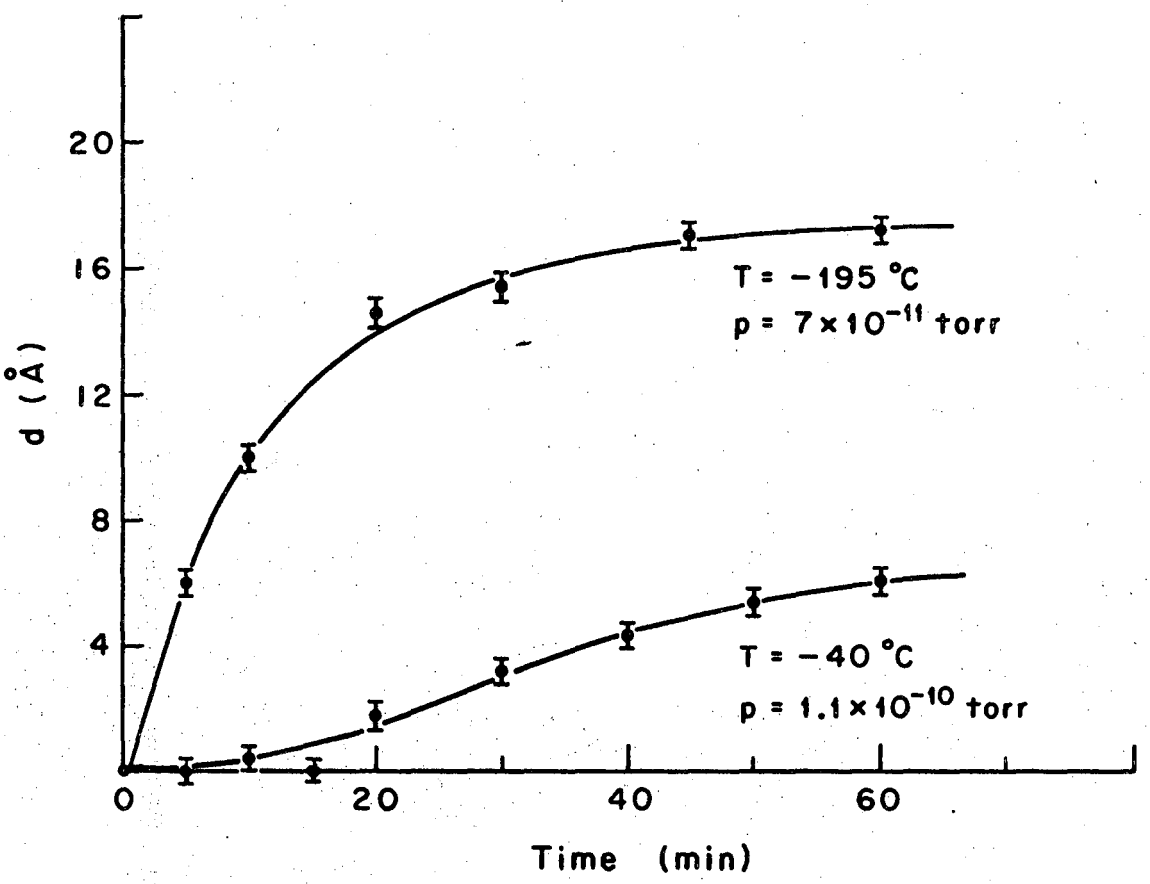

XBL 686-2860-A

Fig. 11

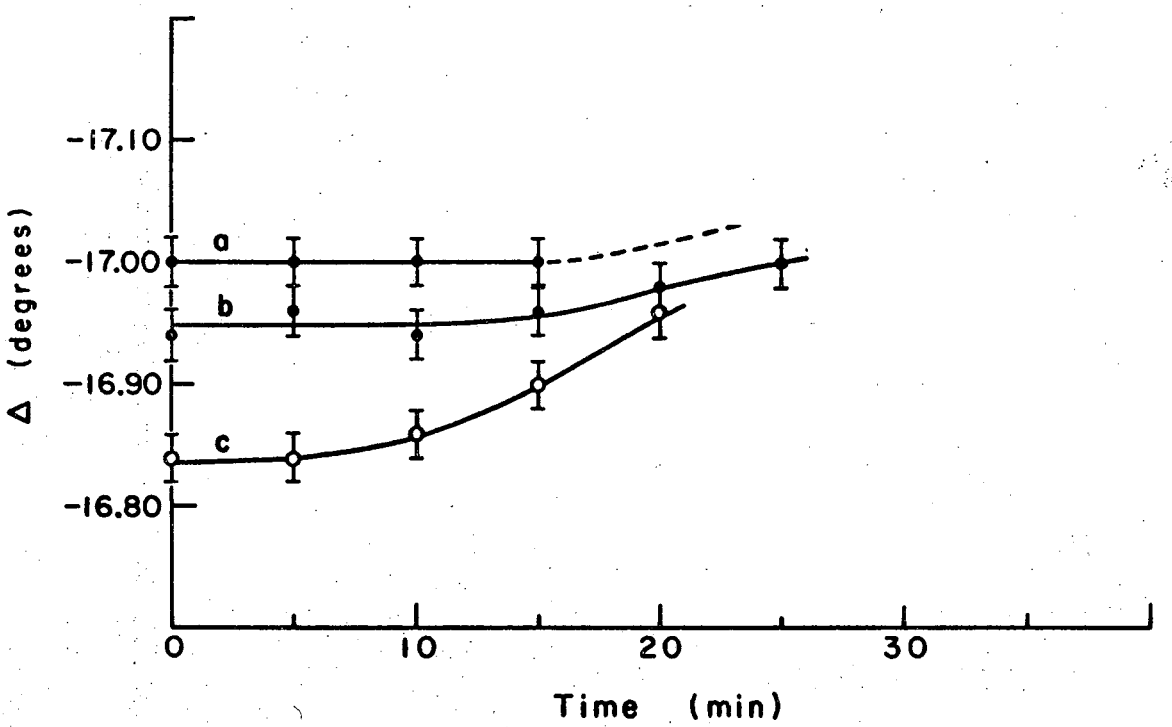

XBL 686-2862-A

Fig. 12

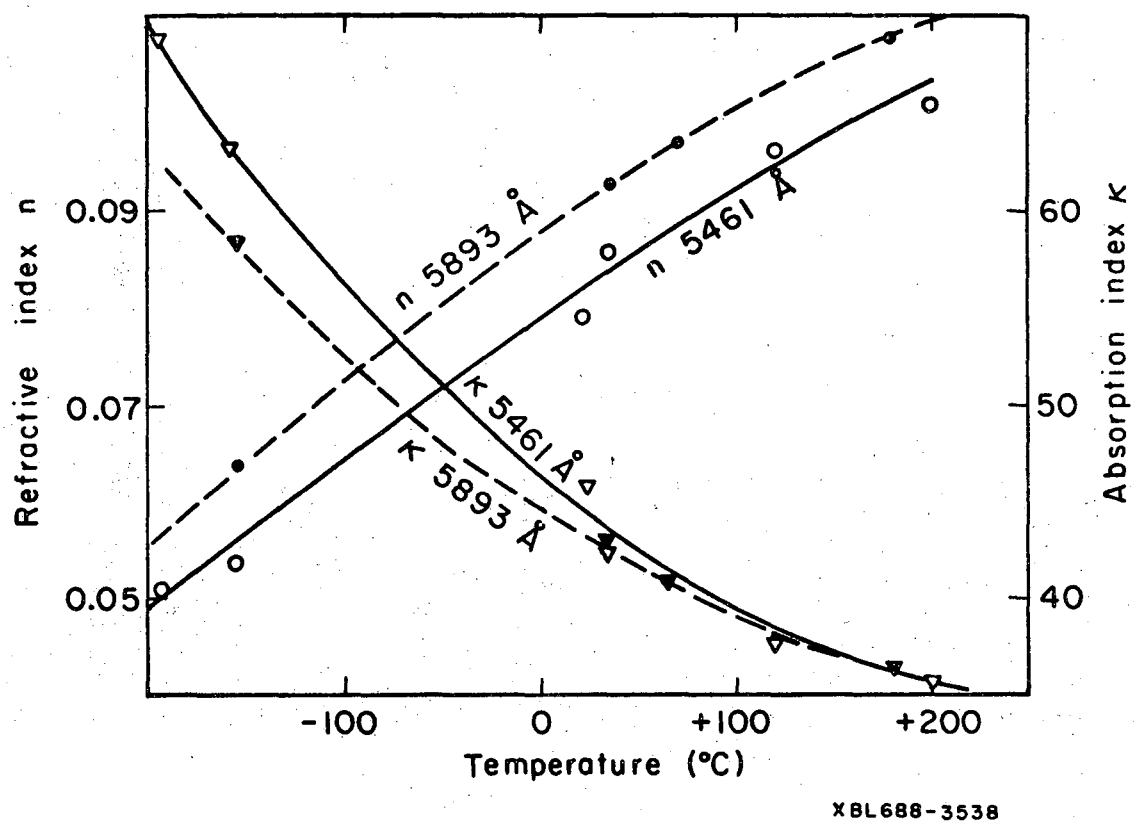
Refractive index n
0.09
0.07
0.05
Absorption index κ
60
50
40
n 5893 Å
n 5461 Å
κ 5461 Å
κ 5893 Å
-100
0
+100
+200
Temperature (°C)
XBL688-3538

Fig. 13

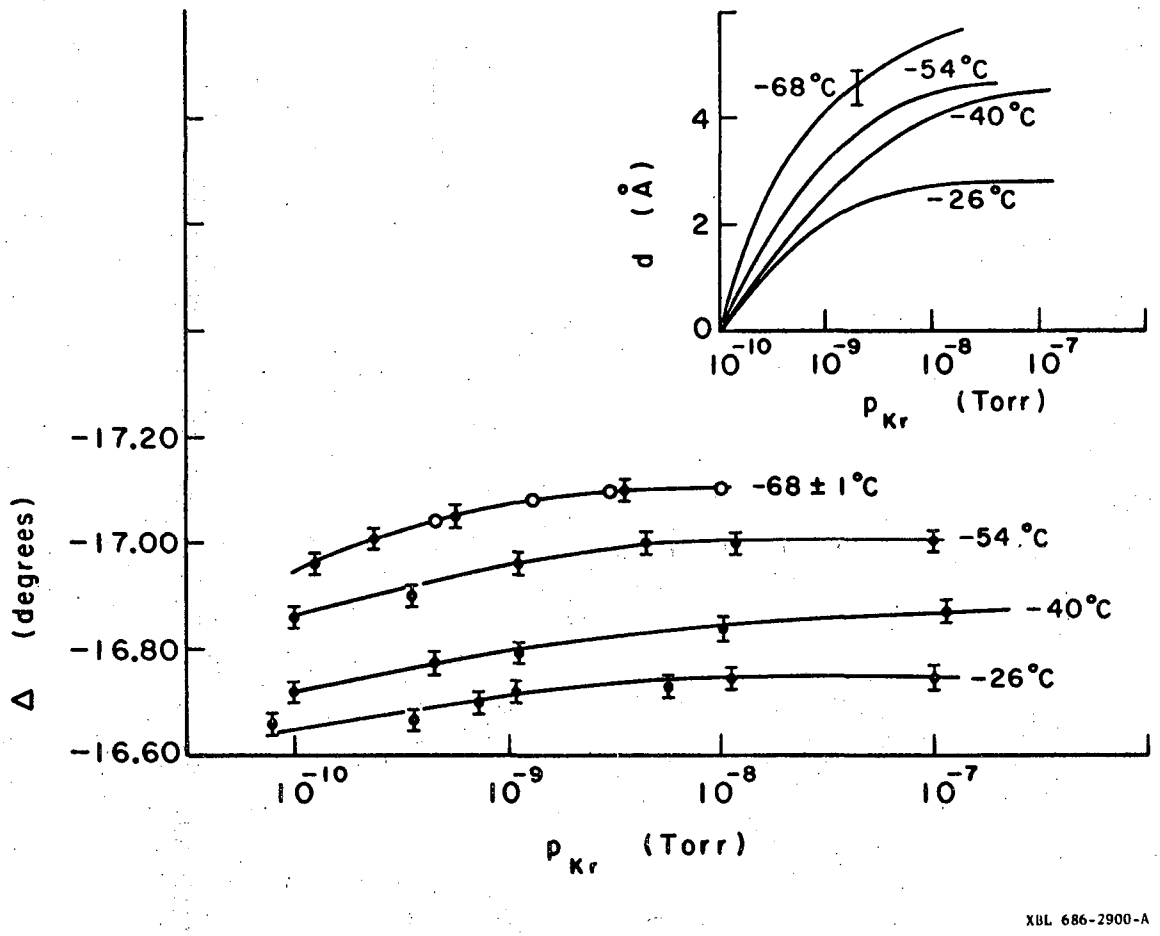

XBL 686-2900-A

Fig. 14a,b

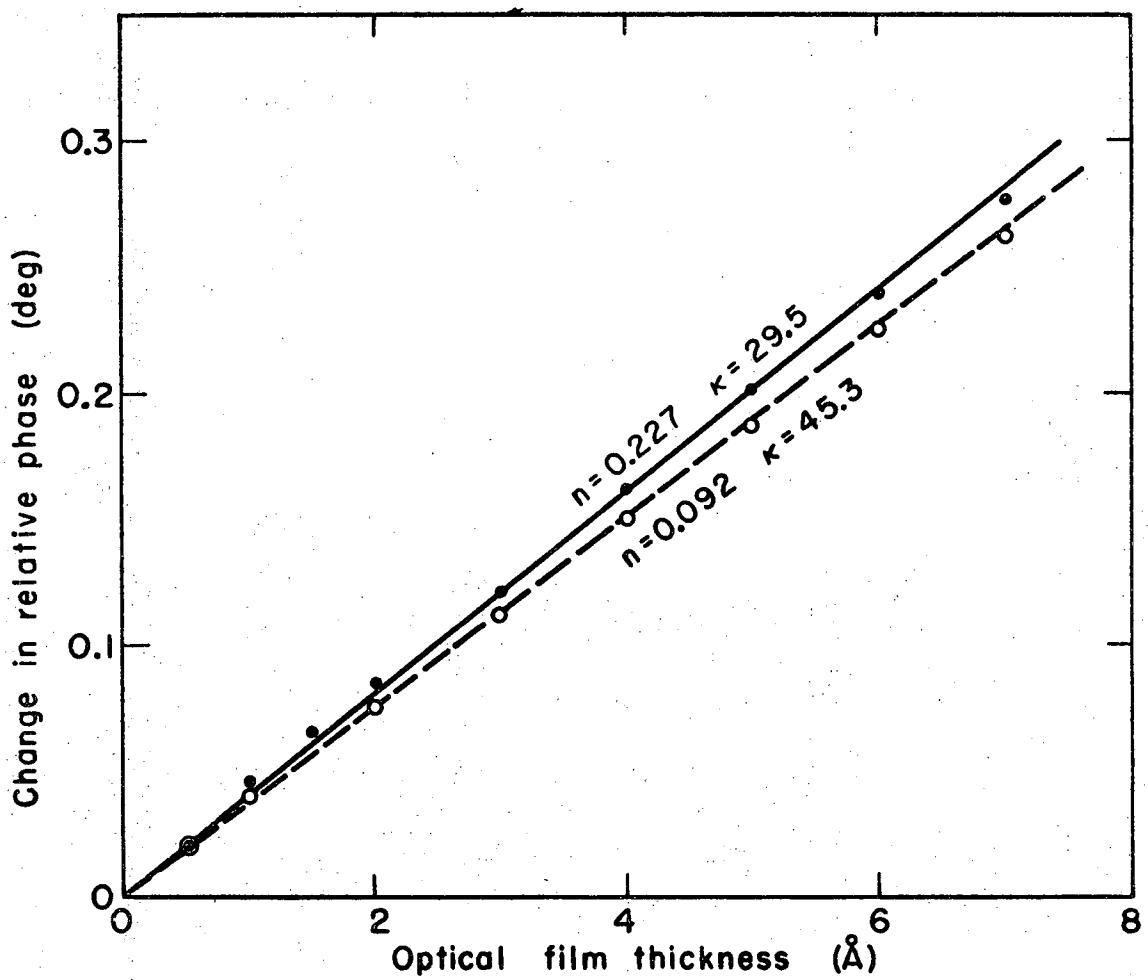

XBL 687-3173-A

Fig. 15

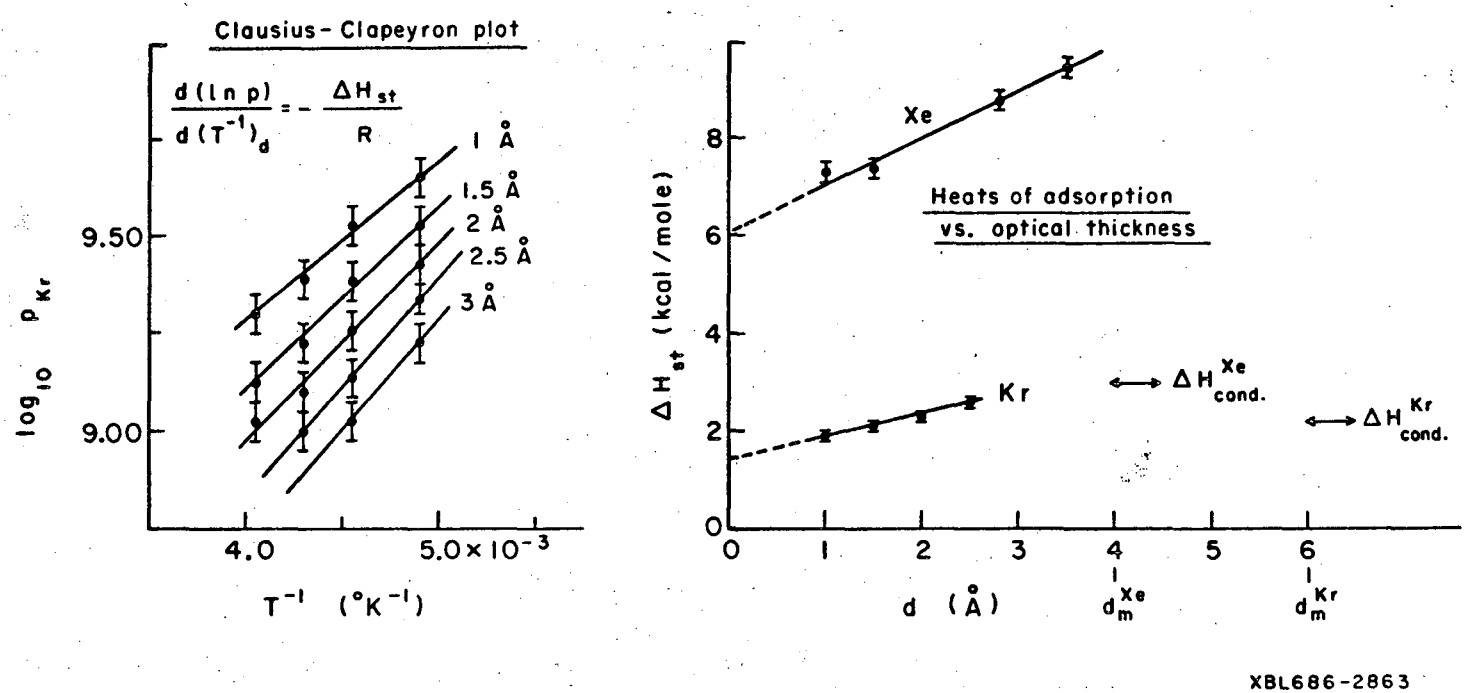
Clausius-Clapeyron plot
$\frac{d(\ln p)}{d(T^{-1})_d} = -\frac{\Delta H_{st}}{R}$
1 Å
1.5 Å
2 Å
2.5 Å
3 Å
9.50
9.00
$\log_{10} p_{Kr}$
4.0
5.0 × 10⁻³
T^{-1} (°K⁻¹)
Heats of adsorption
vs. optical thickness
Xe
Kr
ΔH_{st} (kcal/mole)
$\Delta H^{Xe}_{cond.}$
$\Delta H^{Kr}_{cond.}$
0
2
4
6
8
0
1
2
3
4
5
6
d (Å)
d_m^{Xe}
d_m^{Kr}
XBL686-2863

Fig. 16a,b

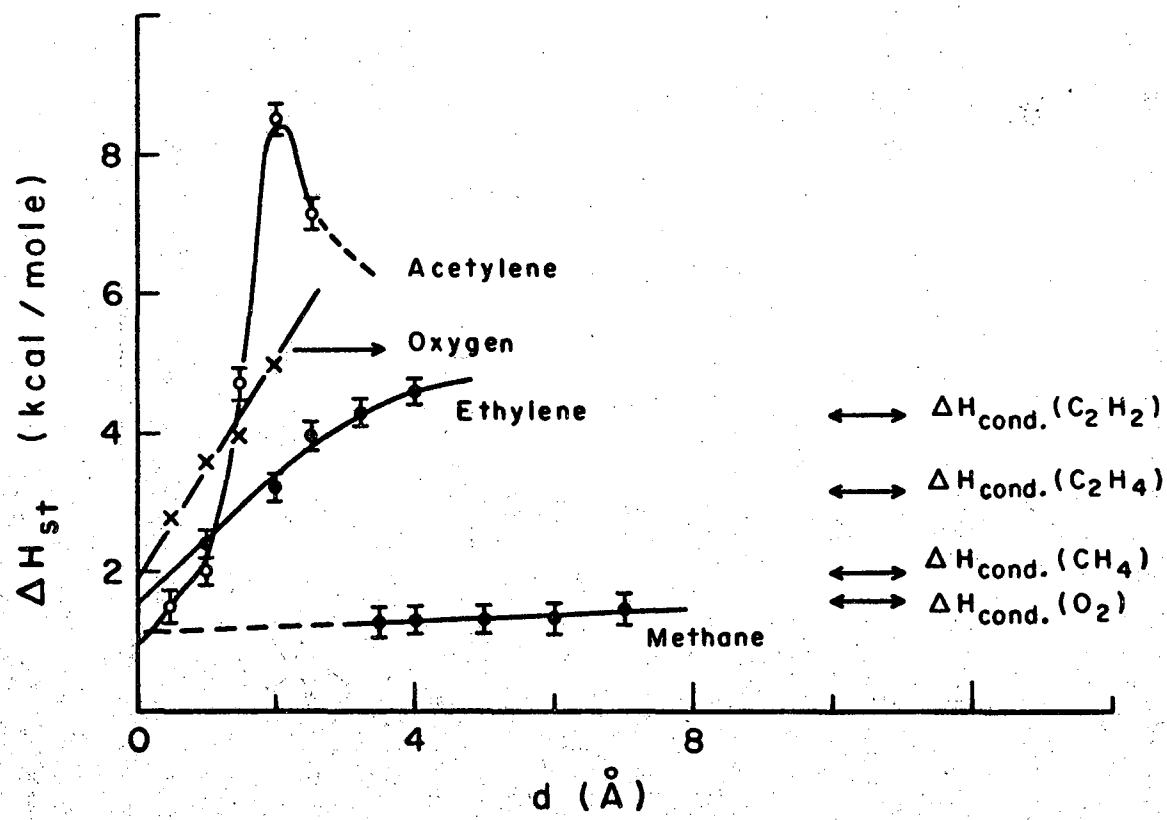

XBL 686-2357-A

Fig. 17

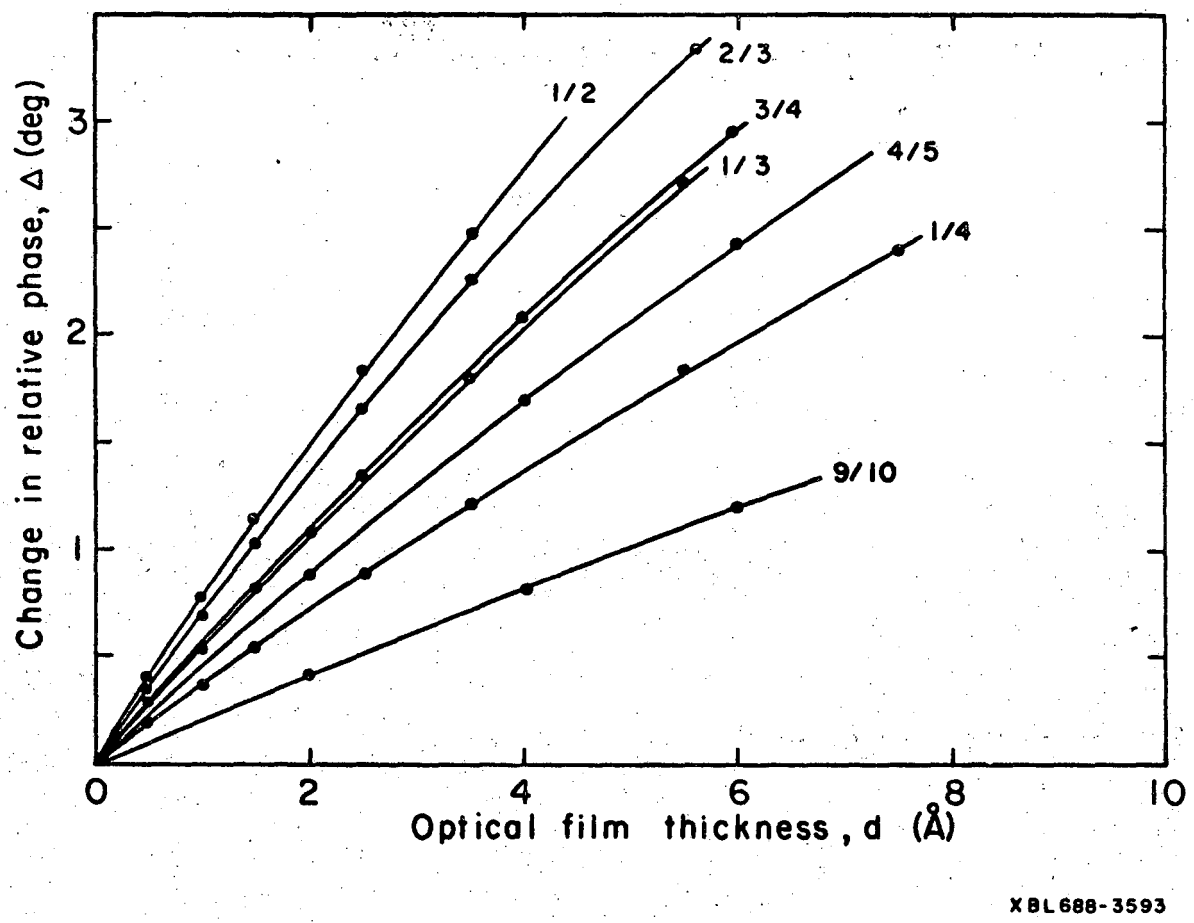
Change in relative phase, Δ (deg)
Optical film thickness, d (Å)
0
2
4
6
8
10
1
2
3
1/2
2/3
3/4
1/3
4/5
1/4
9/10
XBL688-3593

Fig. 18

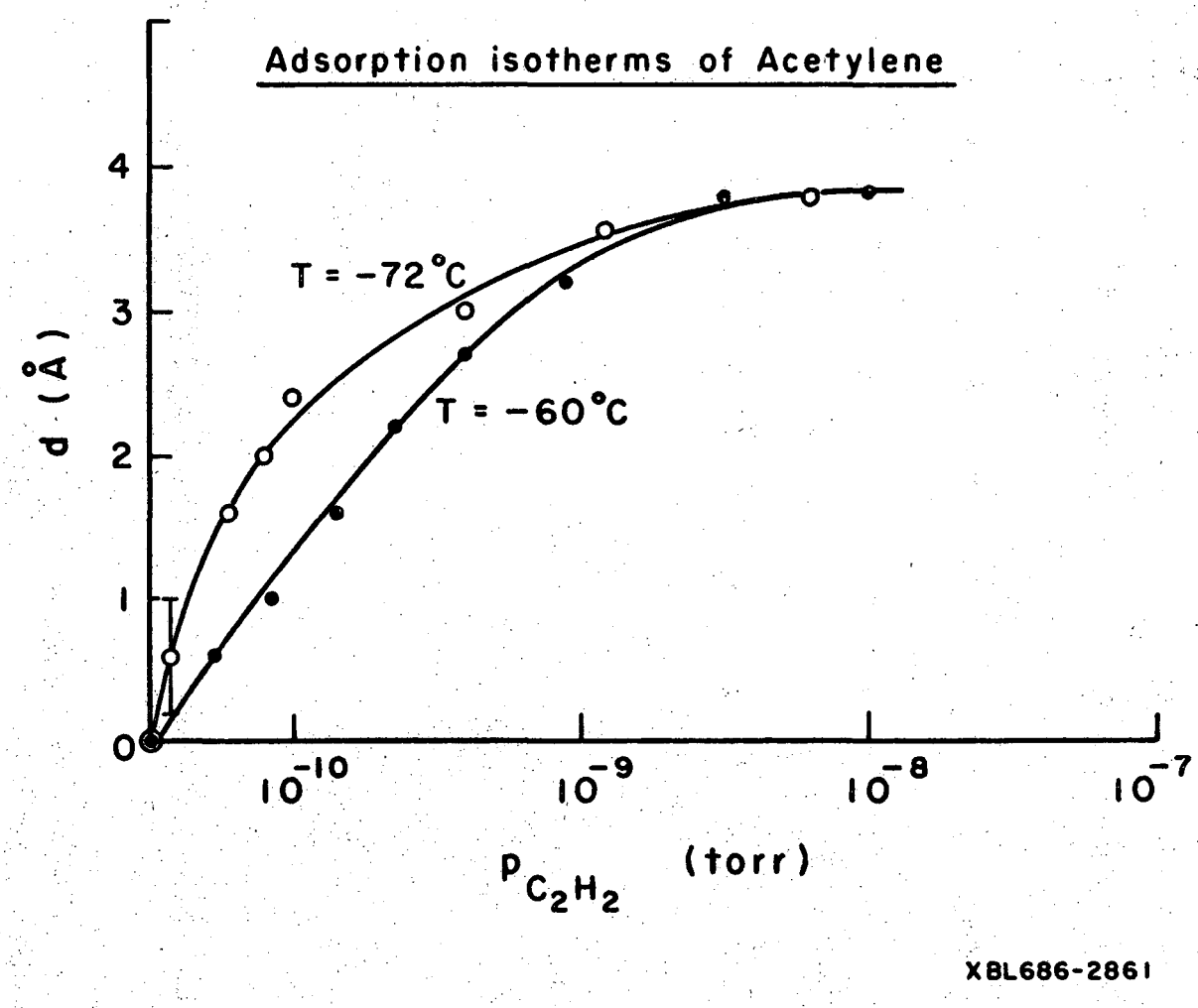
Adsorption isotherms of Acetylene
T = -72°C
T = -60°C
d (Å)
0
1
2
3
4
10^{-10}
10^{-9}
10^{-8}
10^{-7}
$p_{C_2H_2}$ (torr)
XBL686-2861

Fig. 19

LEGAL NOTICE

This report was prepared as an account of Government sponsored work. Neither the United States, nor the Commission, nor any person acting on behalf of the Commission:

A. Makes any warranty or representation, expressed or implied, with respect to the accuracy, completeness, or usefulness of the information contained in this report, or that the use of any information, apparatus, method, or process disclosed in this report may not infringe privately owned rights; or

B. Assumes any liabilities with respect to the use of, or for damages resulting from the use of any information, apparatus, method, or process disclosed in this report.

As used in the above, "person acting on behalf of the Commission" includes any employee or contractor of the Commission, or employee of such contractor, to the extent that such employee or contractor of the Commission, or employee of such contractor prepares, disseminates, or provides access to, any information pursuant to his employment or contract with the Commission, or his employment with such contractor.

TECHNICAL INFORMATION DIVISION
LAWRENCE RADIATION LABORATORY
UNIVERSITY OF CALIFORNIA
BERKELEY, CALIFORNIA 94720